

Ensemble Projections of Regional Climatic Changes over Ontario, Canada

XIUQUAN WANG

Institute for Energy, Environment and Sustainable Communities, University of Regina, Regina, Saskatchewan, Canada

GUOHE HUANG

Institute for Energy, Environment and Sustainability Research, UR–NCEPU, University of Regina, Regina, Saskatchewan, Canada, and Institute for Energy, Environment and Sustainability Research, UR–NCEPU, North China Electric Power University, Beijing, China

JINLIANG LIU

Department of Earth and Space Science and Engineering, York University, Toronto, Ontario, Canada

ZHONG LI AND SHAN ZHAO

Institute for Energy, Environment and Sustainable Communities, University of Regina, Regina, Saskatchewan, Canada

(Manuscript received 9 March 2015, in final form 24 June 2015)

ABSTRACT

In this study, high-resolution climate projections over Ontario, Canada, are developed through an ensemble modeling approach to provide reliable and ready-to-use climate scenarios for assessing plausible effects of future climatic changes at local scales. The Providing Regional Climates for Impacts Studies (PRECIS) regional modeling system is adopted to conduct ensemble simulations in a continuous run from 1950 to 2099, driven by the boundary conditions from a HadCM3-based perturbed physics ensemble. Simulations of temperature and precipitation for the baseline period are first compared to the observed values to validate the performance of the ensemble in capturing the current climatology over Ontario. Future projections for the 2030s, 2050s, and 2080s are then analyzed to help understand plausible changes in its local climate in response to global warming. The analysis indicates that there is likely to be an obvious warming trend with time over the entire province. The increase in average temperature is likely to be varying within [2.6, 2.7]°C in the 2030s, [4.0, 4.7]°C in the 2050s, and [5.9, 7.4]°C in the 2080s. Likewise, the annual total precipitation is projected to increase by [4.5, 7.1]% in the 2030s, [4.6, 10.2]% in the 2050s, and [3.2, 17.5]% in the 2080s. Furthermore, projections of rainfall intensity–duration–frequency (IDF) curves are developed to help understand the effects of global warming on extreme precipitation events. The results suggest that there is likely to be an overall increase in the intensity of rainfall storms. Finally, a data portal named Ontario Climate Change Data Portal (CCDP) is developed to ensure decision-makers and impact researchers have easy and intuitive access to the refined regional climate change scenarios.

1. Introduction

As one of the most pressing issues in the world, climate change has already caused evident impacts on natural and human systems on all continents and across the oceans in

recent decades (IPCC 2014). For example, changing precipitation or melting snow and ice are altering hydrological systems in many regions, which may further affect water resources in terms of quantity and quality (e.g., Crossman et al. 2013; Jordan et al. 2014; Parmesan and Yohe 2003; Piao et al. 2010; Whitehead et al. 2009; Yang and Yang 2014); many terrestrial and marine species have shifted their geographic ranges and migration patterns in response to the ongoing climate change (e.g., Cheung et al. 2009; Doney et al. 2012; Harley et al. 2006;

Corresponding author address: Guohe Huang, Institute for Energy, Environment and Sustainability Research, UR–NCEPU, University of Regina, 3737 Wascana Parkway, Regina SK S4S 0A2, Canada.
E-mail: huang@iseis.org

Ling et al. 2014; Poloczanska et al. 2013; L. Z. Wang et al. 2014); and climate change is also affecting human health as a result of increased frequency and intensity of extreme weather events, including heat waves, floods, and droughts (e.g., Haines et al. 2006; Hansen et al. 2012; Hirabayashi et al. 2013; Ma et al. 2014; McMichael et al. 2006; Patz et al. 2005). This is particularly true for Canada where extreme weather events have frequently struck its major cities in recent years and caused tremendous amounts of damage (He et al. 2011; Robinson et al. 2009; Valeo et al. 2007). For instance, the severe floods in Calgary and Toronto in 2013 have been recorded as the largest natural disasters in the histories of Alberta and Ontario, respectively. The insurance costs caused by these two events have constituted the first and third largest natural insured catastrophes in Canadian history. Recent modeling efforts suggest that continued emission of greenhouse gases will cause further warming and long-lasting changes in all components of the climate system, increasing the likelihood of severe, pervasive, and irreversible impacts on human ecosystems (IPCC 2014). While mitigating climate change would require substantial and sustained reductions in greenhouse gas emissions through worldwide consensus and collaboration, adapting to climate change has become a major focus of regional and local policymakers and development practitioners (Jones et al. 2012; Wende et al. 2012).

Planning adaptation strategies against the changing climate requires a thorough assessment of the potential impacts of climate change at local scales. However, climate change impact assessment is usually subject to a number of challenges that may pose as a barrier to impact researchers and decision-makers. Forecasts of future climate change under different emission scenarios (IPCC 2000; Van Vuuren et al. 2011) can be implemented only with global climate models (GCMs), which usually run at the global scale with a coarse resolution of 150–300 km. This makes GCM outputs unsuitable for driving impact models (e.g., for crops, water resources, and terrestrial ecosystems) because these models require projections with a much finer resolution (in the order of 10 km). Further downscaling through either dynamical or statistical techniques is thus required for deriving regional climate details from the coarse-resolution outputs (e.g., Castro et al. 2005; Diro et al. 2012; Jordan et al. 2014; Pierce et al. 2013; Schmidli et al. 2006; Wang et al. 2013, 2014b). However, effective downscaling of GCM projections is practically difficult for impact researchers because of the lack of computation resources and/or long-term reference data, which are indispensable for either dynamical or statistical downscaling (Fowler et al. 2007; Jha et al. 2013; Rife et al. 2013; Willems et al. 2012). Such difficulty has

become a major barrier preventing informed mitigation and adaptation planning, which is of immediate concern to scientists, practitioners, and policymakers (Bierbaum et al. 2013; Brown and Wilby 2012; Carlsson-Kanyama et al. 2013; Surampalli et al. 2013).

As the largest economy in Canada, the province of Ontario is now suffering extraordinary changes in its local climatology, such as more frequent and intense weather anomalies (e.g., heat waves, floods, droughts, and wind gust) and shorter duration of ice cover on and fluctuating water levels in the Great Lakes. Such changes have caused a large number of weather-related catastrophes along with massive losses of life and tremendous socioeconomic damages (Ontario Ministry of the Environment 2011a). In response to these changes, the government of Ontario has initiated prudent steps to protect its public health, economy, and communities from the harmful effects of climate change (Ontario Ministry of the Environment 2011b). Implementation of such an adaptation initiative substantially depends on our current understanding of future climatic changes in the context of Ontario as well as our confidence about these changes (Wang et al. 2015). As a result, reliable climate projection with finer resolution over Ontario is becoming an urgent need to local policymakers and climate researchers who are focusing on climate change impact assessment at regional scales (Wang et al. 2014a).

In this study, we will develop high-resolution regional climate projections over Ontario using an ensemble modeling approach to provide reliable and ready-to-use climate scenarios for assessing plausible effects of future climatic changes. Specifically, we will adopt the Providing Regional Climates for Impacts Studies (PRECIS) regional climate modeling system to carry out ensemble simulations to the current and future climate over Ontario in a continuous run from 1950 to 2099. The PRECIS ensemble consists of five members that are driven by different boundary conditions from a perturbed physics GCM ensemble based upon the Hadley Centre Coupled Model, version 3 (HadCM3). The simulated results of temperature and precipitation for the baseline period will be compared to the relevant observations to validate the PRECIS ensemble's performance in capturing the current climatology of Ontario. Future projections will then be split into three time slices (i.e., the 2030s, 2050s, and 2080s) to help understand short- and long-term changes in the local climate in response to increasing greenhouse gas emissions. Furthermore, a web-based climate data portal, named Ontario Climate Change Data Portal, will be developed with integration of all modeling results from the PRECIS ensemble to ensure that the public (e.g., decision-makers and impact researchers) have free access to the high-resolution climate projections. Apart from the

representative climate variables, such as temperature, precipitation, humidity, solar radiation, wind speed, and wind direction, we will also develop projections of rainfall intensity–duration–frequency (IDF) curves to help understand the possible effects of climate change on extreme precipitation events. The ensemble projections will be available at various temporal-resolution levels (i.e., annual, seasonal, monthly, daily, and hourly) and thus can be used directly for climate change impact assessment.

2. Methodology

a. Regional climate modeling

In this study, the PRECIS regional climate modeling system developed at the Met Office Hadley Centre is used to generate high-resolution climate projections for the province of Ontario. The PRECIS is a flexible, easy-to-use, and computationally inexpensive RCM designed to provide detailed climate scenarios (Wilson et al. 2011). It can be applied easily to any area of the globe to generate detailed climate change projections, with the provision of a simple user interface as well as a visualization and data-processing package. The PRECIS is able to run at two different horizontal resolutions: 0.44° (approximately 50 km) and 0.22° (approximately 25 km), with 19 vertical levels using a hybrid coordinate system (a combination of σ coordinate and pressure-based coordinate). The PRECIS is a comprehensive physical model with consideration of both the atmosphere and land surface components of the climate system and thus is capable of representing the important physical processes within the climate system, such as dynamical flow, atmospheric sulfur cycle, clouds and precipitation, radiative processes, and the interactions between land surface and deep soil (Jones et al. 2004). Apart from this, a full range of meteorological variables can be diagnosed by the PRECIS model, and its output variables are available at various temporal resolutions (i.e., annual, seasonal, monthly, daily, and hourly).

b. Boundary conditions

Given that RCMs are limited-area models, they need to be driven at their boundaries by time-dependent large-scale fields (e.g., wind, temperature, water vapor, and surface pressure) to provide meteorological forcing for model simulations (Jones et al. 2004). These fields are usually known as boundary conditions and can be derived from either analyses of observations or GCM integrations in a buffer area that is not considered when analyzing the results of the RCM (Bellprat et al. 2012). The PRECIS model requires surface boundary conditions and lateral boundary conditions at its edges, but

there is no prescribed constant at the upper boundary of the model (except for the input of solar radiation). Surface boundary conditions are required only over ocean and inland water where the model needs time series of surface temperatures and ice extents. Lateral boundary conditions provide the necessary dynamical atmospheric information at the latitudinal and longitudinal edges of the model domain (e.g., surface pressure, winds, temperature, and humidity, as well as the necessary chemical species when the sulfur cycle is being modeled). Lateral boundary conditions are updated every 6 h in the PRECIS model, whereas surface boundary conditions are updated every day (Jones et al. 2004).

In this study, we derive boundary conditions from a HadCM3-based perturbed physics ensemble [known as Quantifying Uncertainty in Model Predictions (QUMP); available at <http://www.metoffice.gov.uk/precis/qump>] under the SRES A1B emissions scenario to drive the PRECIS simulations over Ontario. The QUMP consists of 17 members and is developed by the Hadley Centre to allow users to generate an ensemble of high-resolution regional climate projections (Collins et al. 2006; McSweeney et al. 2012). The QUMP ensemble is implemented by varying uncertain parameters in the modeling representation of important physical and dynamical processes. Downscaling the 17-member perturbed physics ensemble (PPE) with PRECIS would require very large inputs of computing resources, data storage, and data analyses. To explore the range of uncertainties while minimizing these requirements, we select five members (i.e., HadCM3Q0, Q3, Q10, Q13, and Q15) from the QUMP ensemble according to the Hadley Centre's recommendation (McSweeney and Jones 2010). HadCM3Q0 is first selected as it is the standard, unperturbed model using the original parameter settings as applied in the atmospheric component of HadCM3. Selection of the remaining four members is based on 1) their performances in simulating the climate of the present day, to ensure that the selected members can represent the climate of the region of interest realistically, and 2) the range or spread of future outcomes, in order to ensure that the selected members can sample the full range of outcomes simulated by the 17-member ensemble (McSweeney et al. 2012). In this study, we perform the PRECIS ensemble simulations in a continuous run from 1950 to 2099 with a resolution of 25 km.

c. Projected IDF curves

The intensity–duration–frequency relationships of rainfall extremes (in the form of IDF curves) are often analyzed and summarized to help understand the characteristics of

extreme rainfall events at given locations. An IDF curve can be generated through a statistical analysis of observed extreme rainfall events to provide the probability of a given rainfall intensity and duration expected to occur at a particular location. IDF curves have been extensively applied in many hydraulic and hydrological engineering practices for the design of structures that control storm water and flooding (e.g., [Borga et al. 2005](#); [Hogg et al. 1989](#); [Madsen et al. 2009](#); [Madsen et al. 2002](#); [Mailhot et al. 2007](#); [Veneziano and Furcolo 2002](#)). However, current development of IDF curves relies on the assumption of a stationary rainfall series such that the intensity and frequency of extreme hydrological events remain unchanged over time ([Mailhot et al. 2007](#)). In fact, such a stationary assumption is not necessarily applicable for future hydrologic time series in the context of climate change ([Chen and Rao 2002](#); [He et al. 2015, 2006](#)). Therefore, we will develop projections of IDF curves using the PRECIS ensemble simulations to help assess the potential impacts of climate change on extreme rainfall events in the context of Ontario. The projected IDF curves will include the frequency of annual extremes of rainfall intensity (mm h^{-1}) or rainfall amount (mm) corresponding to the following durations: 5, 10, 15, 30, and 60 min and 2, 6, 12, and 24 h. As a well-known Type I distribution, Gumbel extreme value distribution will be used to fit the annual extremes such that the extreme rainfall intensity or depth at a given frequency (known as return period, usually expressed in years) can be estimated for all durations. Return periods considered in this study are 2, 5, 10, 25, 50, and 100 yr. The detailed steps for developing the projected IDF curves are provided in the work of [Wang et al. \(2014c\)](#).

d. Ensemble percentiles

To synthesize the ensemble simulations by the PRECIS model, we use the Type 7 algorithm ([Hyndman and Fan 1996](#)) hereinafter to derive quantiles (or percentiles) through a piecewise linear interpolation. To allow for more freedom in exploring the uncertainties associated with the simulations, we calculate the following ensemble percentiles: 10th, 20th, 30th, . . . , 80th, and 90th. Following the approach used in the UK Climate Projections report ([Murphy et al. 2009](#)), we select three typical percentiles (i.e., 10th, 50th, and 90th) to summarize the possible outcomes of future projections. In detail, the median (viz., the 50th percentile) is used here to represent the central value of the distribution, indicating that half of the members are less than or equal to it; the 10th percentile is used to describe the ensemble projections as very likely to be greater than or very unlikely to be less than, while the 90th percentile is to indicate very likely to be less than or very unlikely to be greater than.

3. Development of Ontario CCDP

A web-based data portal, known as Ontario Climate Change Data Portal (CCDP), is developed to make the ensemble regional climate change projections available to the public (at <http://ontarioccdp.ca>). Ontario CCDP is implemented with provision of both visual representations and data downloading functions of climate scenarios using geospatial maps in order to ensure that technical or nontechnical end users (e.g., municipalities, private sectors) have easy and intuitive access to the refined Ontario-focused high-resolution regional climate data.

a. Framework and functionality

As outlined in [Fig. 1](#), Ontario CCDP consists of five modules: user access, map overview, IDF curves, time series downloading, and help center. The user access module is designed to facilitate quick and easy access to the datasets of Ontario CCDP. The access to Ontario CCDP is free of charge, but users are required to create an account through user registration while downloading data. Only basic information (e.g., name, organization, and research purpose) will be collected for statistical purposes. The map overview module consists of map selector, map layer controller, and panel controller, which is developed with the up-to-date web-based technologies and online map visualization tools (i.e., ArcMap version 10 and ArcGIS Online: <http://www.esri.com/software/arcgis/arcgisonline>). It allows users to view high-resolution maps of climate projections (e.g., for temperature and precipitation) over Ontario quickly and easily, and it only requires an Internet browser. Free access to IDF curves is also implemented with the aid of the IDF curves selector and viewer, which enables users to preview IDF curves for each 25-km grid cell and to download the corresponding data file for further analysis. The time series downloading module is the most challenging but also the most useful function of Ontario CCDP because of its huge data volume (~4 terabytes), including daily and hourly time series spanning from 1960 to 2095 for up to seven climate variables. With the integration of the variable selector and grid data downloader, it allows users to easily locate and download the time series at specific points or regions of interest. The time series included in Ontario CCDP can be used directly for driving impact models to help assess the impacts of climatic changes at regional scales. In addition, Ontario CCDP provides an online help center, including an “About Us” page, frequently asked questions, and contact information, to provide necessary documentation and guidance regarding the use of the data portal.

The home page of Ontario CCDP is designed with a neat and user-friendly layout (shown in [Fig. 2](#)). Users

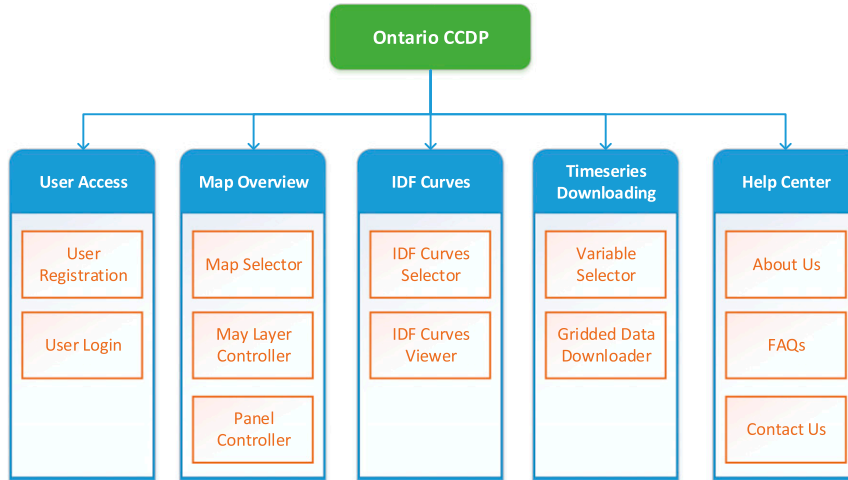


FIG. 1. Framework of Ontario CCDP.

can explore freely more than 1200 gridded maps to help illustrate the spatial patterns of temperature and precipitation projections over Ontario. The main panel serves as a main controller allowing users to select the climate variable, time period, measurement, and averaging options as well as the ensemble percentile. One can also switch on or off a number of map layers (including Ontario boundary, census divisions, census subdivisions, census tracts, agriculture regions, and

health regions) and other information panels (such as the gauge panel, legend panel, and cursor panel) to facilitate the exploration of the high-resolution climate projections included by Ontario CCDP. Additionally, a number of auxiliary functions are provided to help with map viewing and data downloading. For example, the map view controller enables users to change the transparency of the gridded map, find users' geographical location, reset the map to default extent, and zoom in

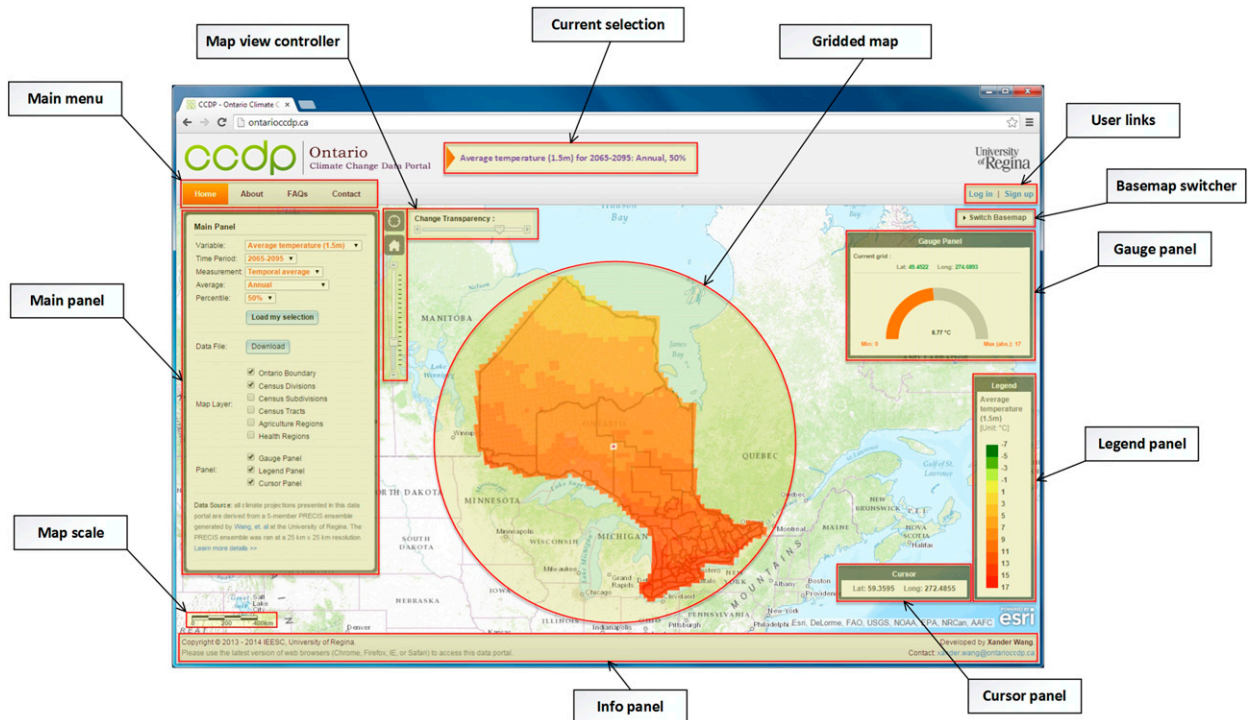


FIG. 2. The home page layout of Ontario CCDP.

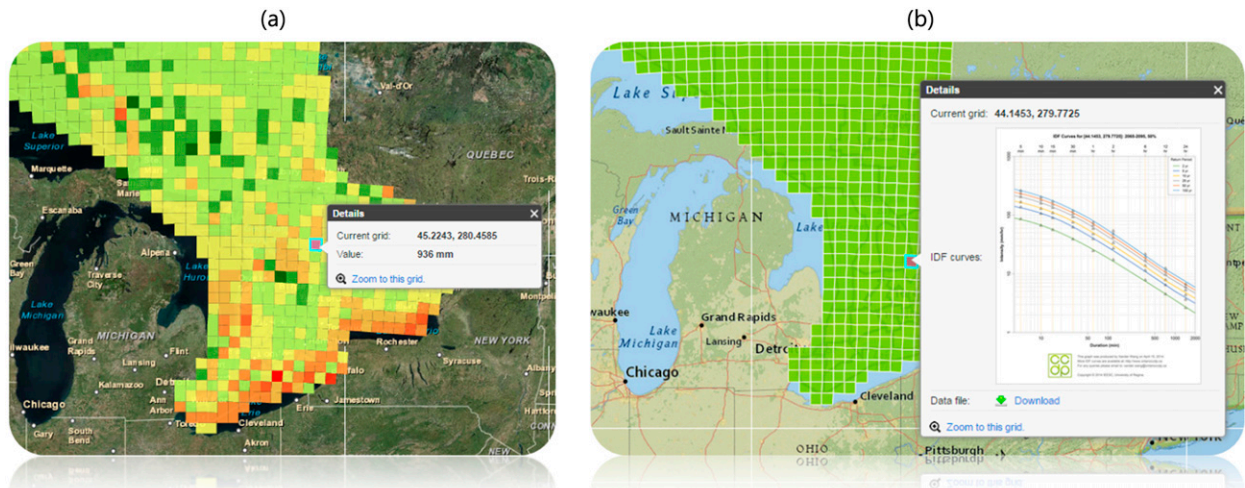


FIG. 3. Examples with different base maps: (a) annual precipitation for the 2080s (50th percentile) with imagery base map; (b) projected IDF curves for the 2050s (50th percentile) with National Geographic base map.

and out on the map; base map switcher allows users to choose an appropriate basemap to help analyze the spatial variations and local patterns of the projections (see the examples shown in Fig. 3).

b. Climate data integration

As a physically based model, the PRECIS outputs a full range of meteorological variables at various temporal resolutions. Because of the huge data volume, only a small number of output variables are provided in Ontario CCDP. Temperature and precipitation are included as they are widely regarded as indicators of climate change. In addition, another five variables of wide concern for climate impact researchers (i.e., relative humidity, surface solar radiation, wind speed, and wind components U and V) are incorporated to provide driving scenarios for impact models. The data availability for climate variables and IDF curves is detailed in

Table 1. Projections for daily average temperature and total precipitation are available for four time periods (i.e., baseline period, 2030s, 2050s, and 2080s) at all temporal resolutions (i.e., annual, seasonal, monthly, daily, and hourly). For the remaining variables, we provide time series only for either daily or hourly time steps. The projections of IDF curves are also available for four time periods. Note that the datasets provided in the platform cover ~ 1900 $25\text{ km} \times 25\text{ km}$ grid cells over the province of Ontario.

4. Results

a. Validation of the PRECIS ensemble

We use the 10-km gridded climate dataset provided by the National Land and Water Information Service (NLWIS) Agriculture and Agri-Food Canada to validate the capability of the PRECIS ensemble simulations in capturing the historical climatology of Ontario. The

TABLE 1. Climate data provided by Ontario CCDP. Note that the check mark indicates that data for this combination are available while a dash indicates that data are either not applicable or not available.

| Variable | Unit | Time period | | | | Temporal average | | | Time series | |
|---------------------------|--------------------|-------------|-------|-------|-------|------------------|----------|---------|-------------|--------|
| | | Baseline | 2030s | 2050s | 2080s | Annual | Seasonal | Monthly | Daily | Hourly |
| Daily avg temp (1.5 m) | $^{\circ}\text{C}$ | ✓ | ✓ | ✓ | ✓ | ✓ | ✓ | ✓ | ✓ | ✓ |
| Daily max temp (1.5 m) | $^{\circ}\text{C}$ | ✓ | ✓ | ✓ | ✓ | — | — | — | ✓ | — |
| Daily min temp (1.5 m) | $^{\circ}\text{C}$ | ✓ | ✓ | ✓ | ✓ | — | — | — | ✓ | — |
| Total precipitation | mm | ✓ | ✓ | ✓ | ✓ | ✓ | ✓ | ✓ | ✓ | ✓ |
| Relative humidity (1.5 m) | % | ✓ | ✓ | ✓ | ✓ | — | — | — | — | ✓ |
| Surface solar radiation | W m^{-2} | ✓ | ✓ | ✓ | ✓ | — | — | — | — | ✓ |
| Wind speed (10 m) | m s^{-1} | ✓ | ✓ | ✓ | ✓ | — | — | — | — | ✓ |
| Wind component U (10 m) | m s^{-1} | ✓ | ✓ | ✓ | ✓ | — | — | — | — | ✓ |
| Wind component V (10 m) | m s^{-1} | ✓ | ✓ | ✓ | ✓ | — | — | — | — | ✓ |
| IDF curves | — | ✓ | ✓ | ✓ | ✓ | — | — | — | — | — |

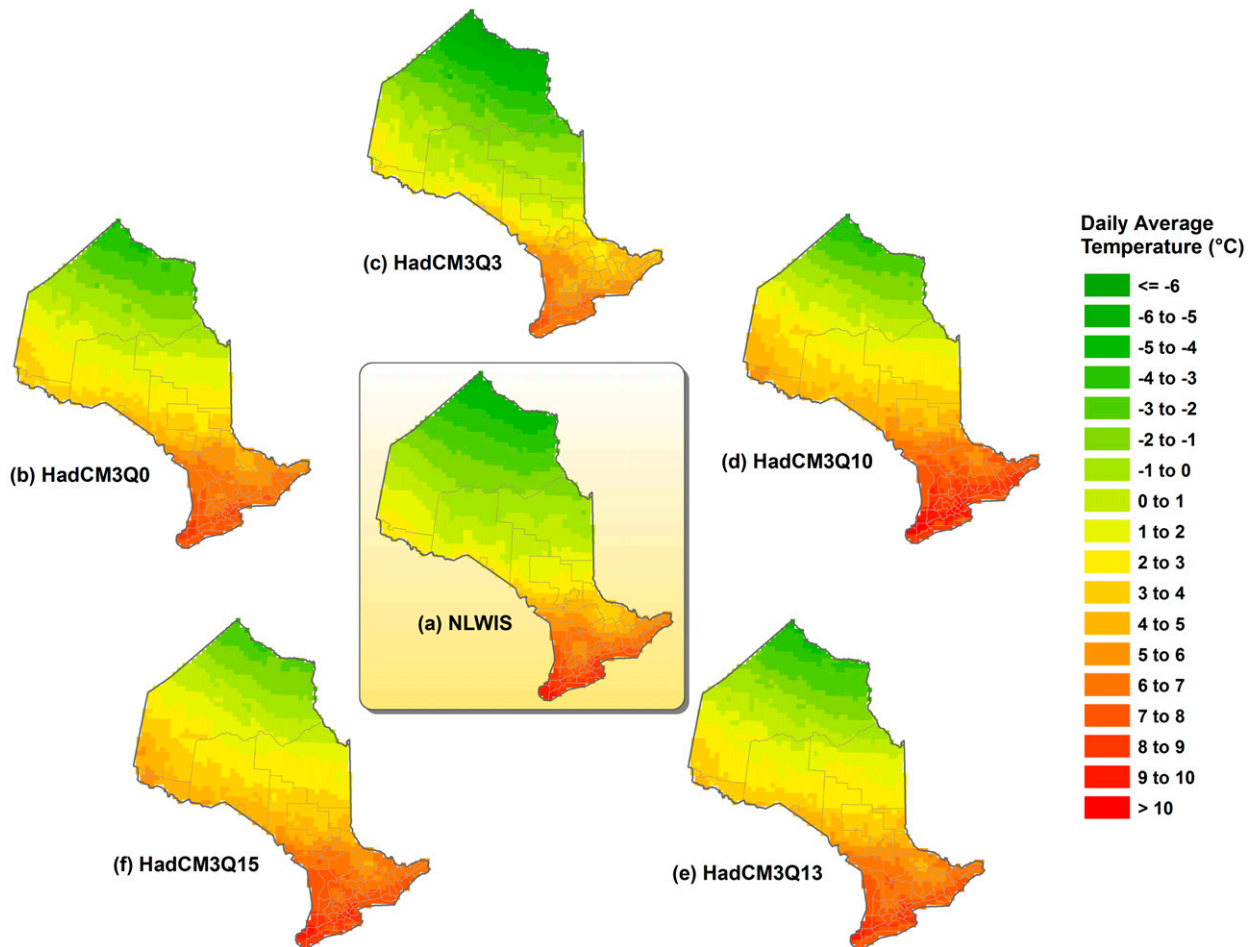


FIG. 4. Comparison of daily average temperature between (a) the NLWIS dataset and (b)–(f) the ensemble members.

NLWIS dataset is interpolated from daily Environment Canada climate station observations through a thin-plate smoothing spline surface fitting method as implemented by the thin plate spline smoothing algorithms (ANUSPLIN), version 4.3 (NLWIS 2007). The NLWIS dataset contains daily maximum temperature, minimum temperature, and precipitation for 1961–2003 covering the Canadian landmass south of 60°N. Here we estimate daily average temperature on each 10-km grid cell using the average of daily maximum and minimum temperature. The data for 1961–90 is extracted to represent the observations of historical climate in the context of Ontario. The NLWIS dataset is regridded to the 25-km grids of the PRECIS model such that the undermentioned validation analyses can be conducted at the same spatial resolution.

We first evaluate the performance of each member of the ensemble by comparing each one with the NLWIS dataset separately. Figures 4 and 5 show the comparisons of daily average temperature and annual total precipitation. Here we use the name of its driving

boundary condition to denote each member in order to distinguish it from the others. It seems that most of the ensemble members (i.e., HadCM3Q0, Q10, Q13, and Q15) are likely to slightly overestimate the daily average temperature in the baseline period. This is especially true for the central and northern areas of Ontario. Specifically, the simulated average temperature by these four members is mostly bounded by [1, 4]°C in the middle and [−3, 1]°C in the north, while the observed average temperature is mainly ranging within [−1, 3]°C in the middle and [−5, −1]°C in the north. As for the average temperature over southern Ontario, these four members show good agreement with the observations except for the Q10 member, which presents apparent warm bias in most of the area. By contrast, the Q3 member shows better performance in capturing the spatial pattern of daily average temperature than these four members, even though it tends to slightly underestimate the observed daily average temperature in the north and south. Not surprisingly, the ensemble

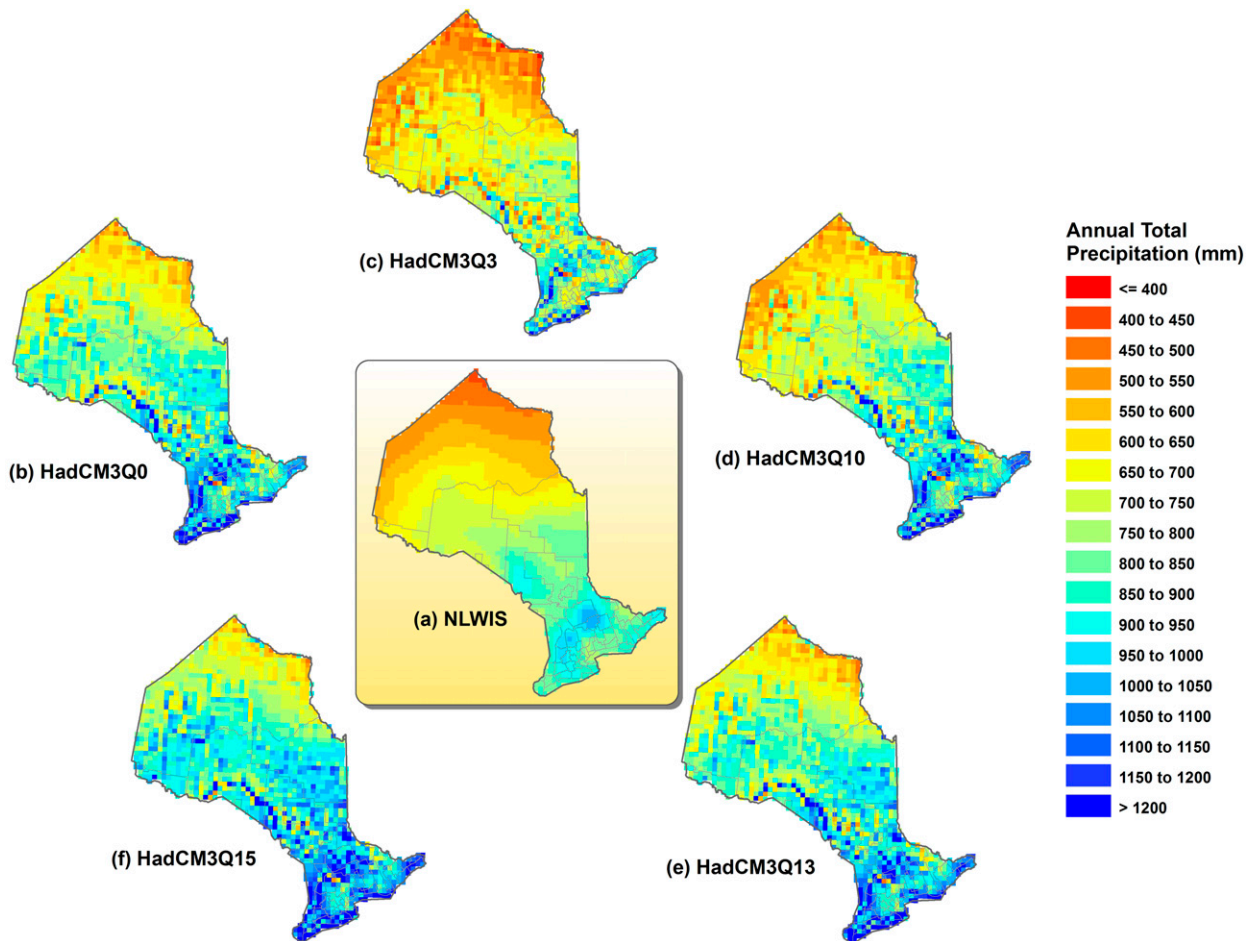


FIG. 5. As in Fig. 4, but for annual total precipitation.

members demonstrate similar performance in simulating the annual total precipitation. The Q3 member shows satisfactory performance in reflecting the spatial pattern of precipitation in comparison with the other four members, which are all likely to generate more precipitation than the observations. In addition, we notice that all the ensemble members perform very well in reflecting the spatial variations in precipitation at a higher resolution, while the NLWIS dataset can hardly do so because of its basis on a smoothing interpolation algorithm. Based on the initial performance evaluation to each member of the PRECIS ensemble, it is apparent that the Q3 member performs the best in hindcasting both temperature and precipitation. However, it is not suggested to use the results only from this member for the subsequent impact assessment because it can hardly reflect the uncertainties associated with the future climate projections.

To investigate the overall performance of the ensemble simulations in capturing the historical climatology over

Ontario, we further compare three typical percentiles (i.e., 10th, 50th, and 90th) of the ensemble with the NLWIS dataset. Apart from daily average temperature and annual total precipitation, our comparisons also cover daily maximum and minimum temperature as well as seasonal total precipitation. The comparisons are presented as the difference between the ensemble percentiles and the NLWIS dataset. Figure 6 shows differences in daily average, maximum, and minimum temperature. The 10th percentiles of difference in average temperature over the entire province are mainly ranging within $[-1, 1]^{\circ}\text{C}$, while its 90th percentiles are largely bounded by $[1, 3]^{\circ}\text{C}$. This means that the observations of average temperature are mostly bounded by the 10th and 90th percentiles of the PRECIS ensemble, indicating that the ensemble simulations are capable of hindcasting the average temperature over Ontario in the baseline period. Similarly, the ensemble simulations also perform well in capturing daily maximum temperature as the 10th percentiles

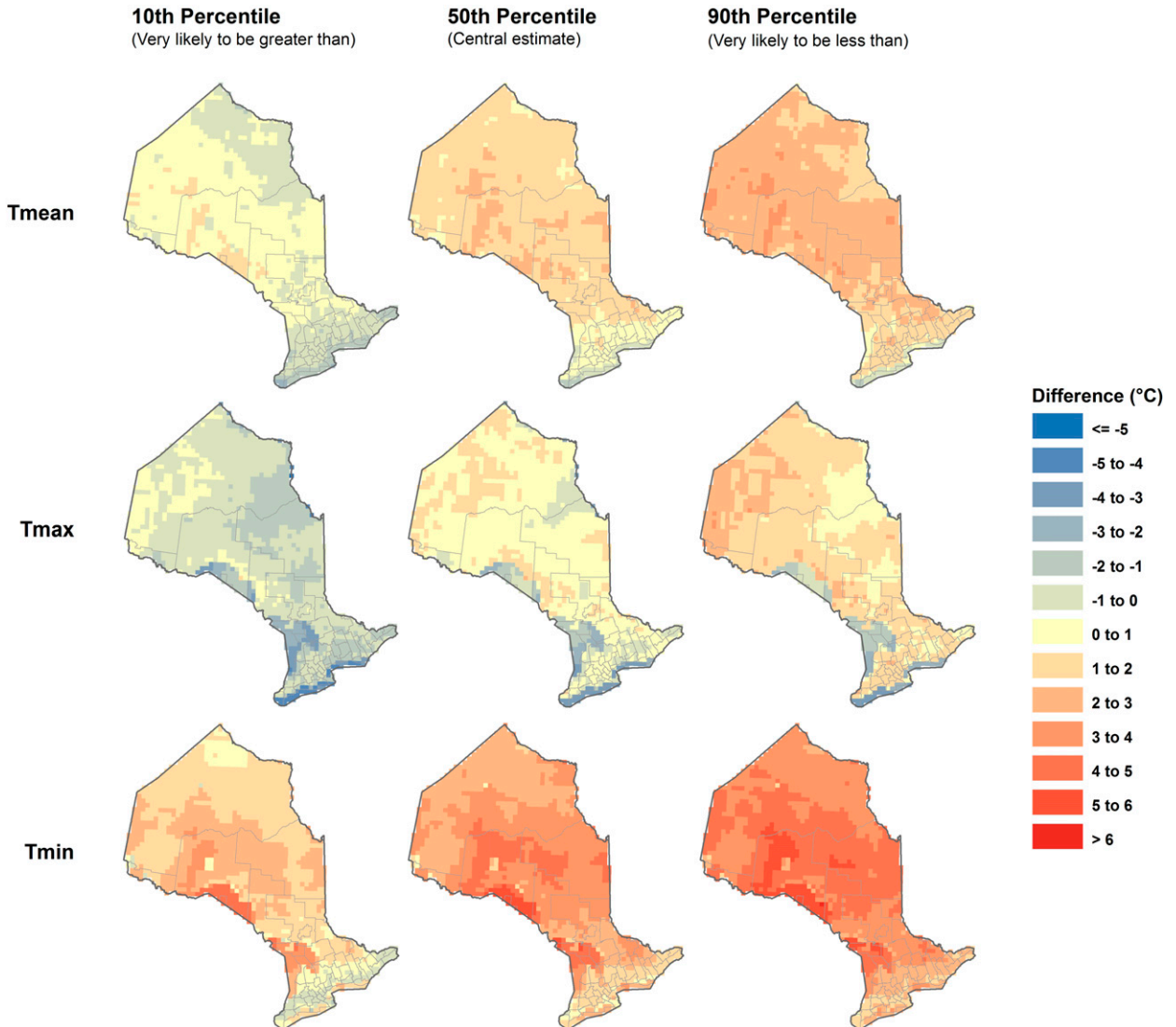


FIG. 6. Difference in daily (top) average, (middle) maximum, and (bottom) minimum temperature between the ensemble simulations and the NLWIS dataset: (left)–(right) 10, 50, and 90th percentiles.

of difference mainly vary within $[-2, 0]^{\circ}\text{C}$ and the 90th percentiles of difference are mostly within $[0, 2]^{\circ}\text{C}$. However, apparent negative differences in daily maximum temperature are found over the Great Lakes. This may suggest that the PRECIS model is likely to underestimate the maximum near-surface air temperature over the Great Lakes. It seems that the ensemble simulations perform relatively poorly in hindcasting daily minimum temperature because its 10th percentiles of difference mainly vary within $[1, 3]^{\circ}\text{C}$ over most areas of Ontario, except for the southern end where the 10th percentiles of difference are largely bounded by $[-1, 1]^{\circ}\text{C}$. In addition, the obvious warm bias over the Great Lakes may suggest that the PRECIS model is

likely to overestimate the minimum near-surface temperature over large bodies of inland water.

Figure 7 shows the differences in annual and seasonal precipitation between the ensemble simulations and the NLWIS dataset. The 10th percentiles of difference in winter, summer, and autumn precipitation are mostly negative, while their 90th percentiles of difference are primarily positive within the domain of Ontario, demonstrating the reasonable performance of the ensemble simulations in capturing the historical precipitation patterns in these three seasons. By contrast, the 10th percentiles of difference in spring precipitation show apparent positive bias over most areas of Ontario. This is especially true for the north and the middle regions

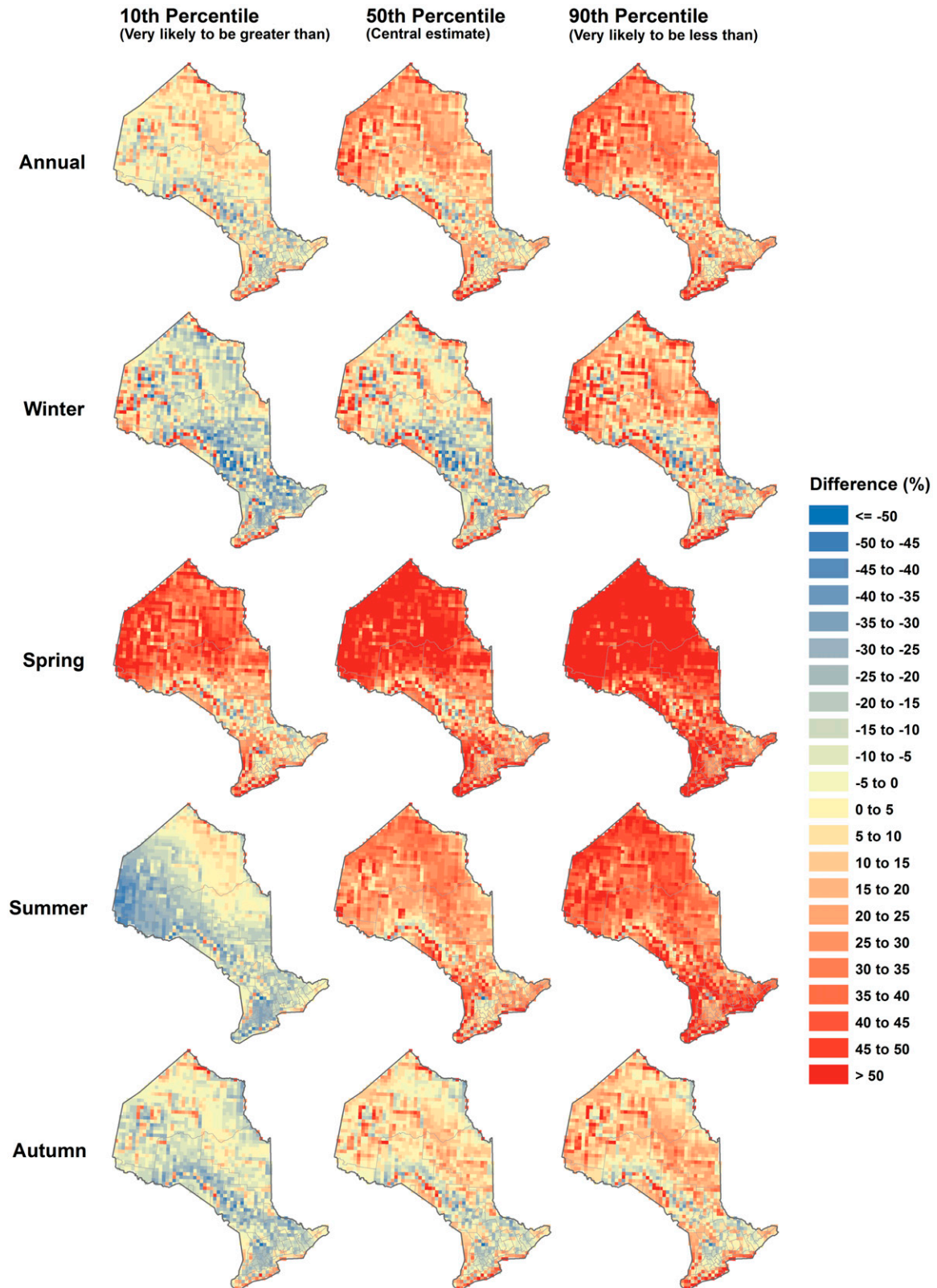


FIG. 7. Difference in (top)–(bottom) annual and seasonal total precipitation between the ensemble simulations and the NLWIS dataset: (left)–(right) 10, 50, and 90th percentiles.

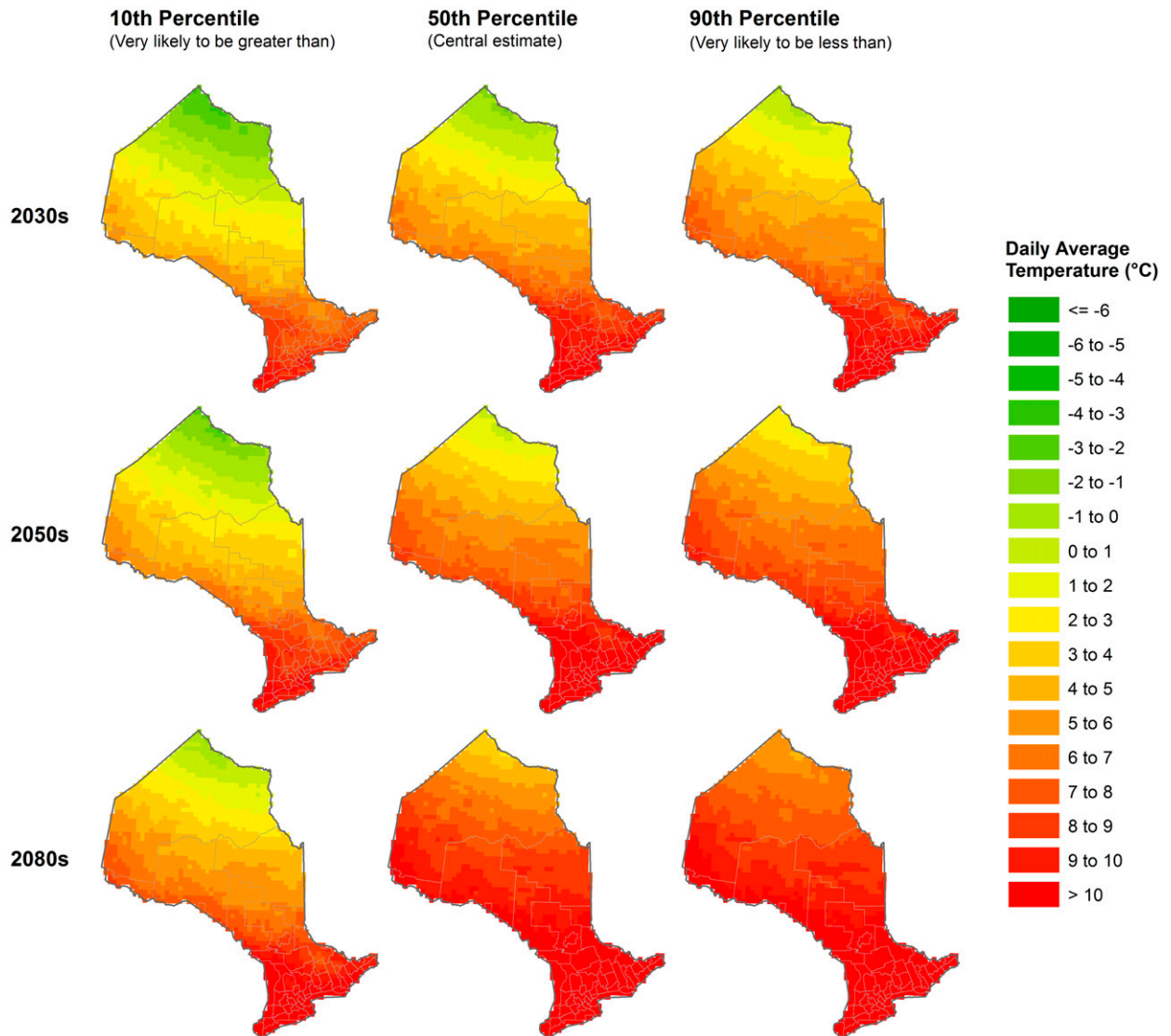


FIG. 8. Projections of daily average temperature for (top)–(bottom) 2030s, 2050s, and 2060s over Ontario and (left)–(right) 10, 50, and 90th percentiles.

where the bias in precipitation can be as high as [25, 35]%. This may suggest that the PRECIS model is likely to generate more precipitation in spring in the baseline period. Such positive bias in spring precipitation more or less affect the annual total precipitation, although the ensemble simulations perform generally well in simulating precipitation of the other three seasons. In detail, the 10th percentiles of difference in annual total precipitation are largely bounded by [0, 10]% in the north and are primarily bounded by [−15, 0]% in the south, while the 90th percentiles of difference in annual total precipitation are mostly positive. This indicates that the ensemble simulations are capable of capturing the annual precipitation patterns in the

south but are likely to slightly overestimate the annual precipitation in the north.

b. Future climate projections

Ensemble projections for a number of climate variables are provided in Ontario CCDP; here we present only the results of daily average temperature and annual and seasonal total precipitation. Figure 8 shows the projections of daily average temperature over Ontario for three future 30-yr periods at the 10th, 50th, and 90th percentiles. It seems that there is likely to be an obvious warming trend with time over the entire province. This is especially true for the northern end where the central estimate of average temperature is projected to be

TABLE 2. Information of the selected cities.

| No. | City name | Longitude | Latitude |
|-----|---------------|-----------|----------|
| 1 | Fort Hope | 87°54'W | 51°34'N |
| 2 | Fort Severn | 87°38'W | 56°00'N |
| 3 | Kenora | 94°29'W | 49°46'N |
| 4 | Marathon | 86°23'W | 48°43'N |
| 5 | Moose Factory | 80°36'W | 51°16'N |
| 6 | Ottawa | 75°41'W | 45°24'N |
| 7 | Sudbury | 81°00'W | 46°29'N |
| 8 | Toronto | 79°23'W | 43°39'N |
| 9 | Windsor | 83°03'W | 42°18'N |

below zero (i.e., $[-2, 0]^{\circ}\text{C}$) in the 2030s; afterward the average temperature is likely to rise above zero (i.e., $[0, 2]^{\circ}\text{C}$) in the 2050s and would continue to increase and reach up to $[3, 5]^{\circ}\text{C}$ in the 2080s. To further analyze the projected warming trend across the province, we choose nine representative cities that are geographically located

across the landmass of Ontario. Information about the selected cities is listed in Table 2. We extract the projections of daily average temperature in three future periods as well as the simulations of the baseline period for these nine cities and then compare their changes in temperature relative to the baseline period. The results are presented in Fig. 9. It is interesting to find that there is no big difference in the magnitude of the temperature increase among the selected cities even though their projected values of daily average temperature may significantly differ from each other. For example, the average temperature in the most northern city (i.e., Fort Severn) is projected to be -1.2°C in the 2030s, while the temperature for the same period in the most southern city (i.e., Windsor) would be as high as 12.1°C . However, they are likely to suffer the same change in average temperature (i.e., $+2.7^{\circ}\text{C}$) in the 2030s. For all cities, the projected increases in average temperature would be

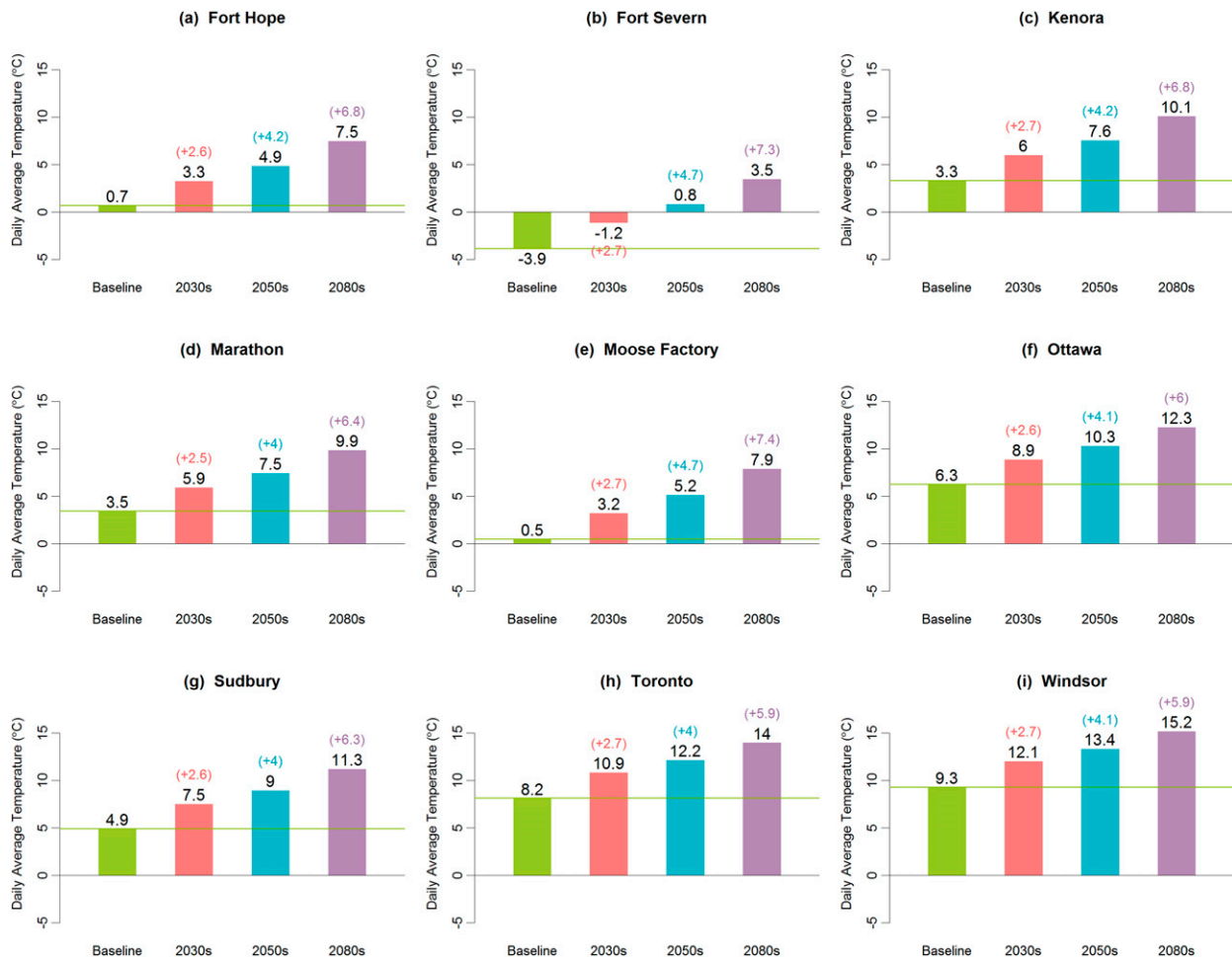


FIG. 9. Projected increases in daily average temperature at (a)–(i) selected cities (50th percentile) from baseline values to values in the 2030s, 2050s, and 2080s. The values in parentheses indicate the changes in daily average temperature relative to the baseline period. The plus and minus signs indicate increase and decrease in temperature, respectively.

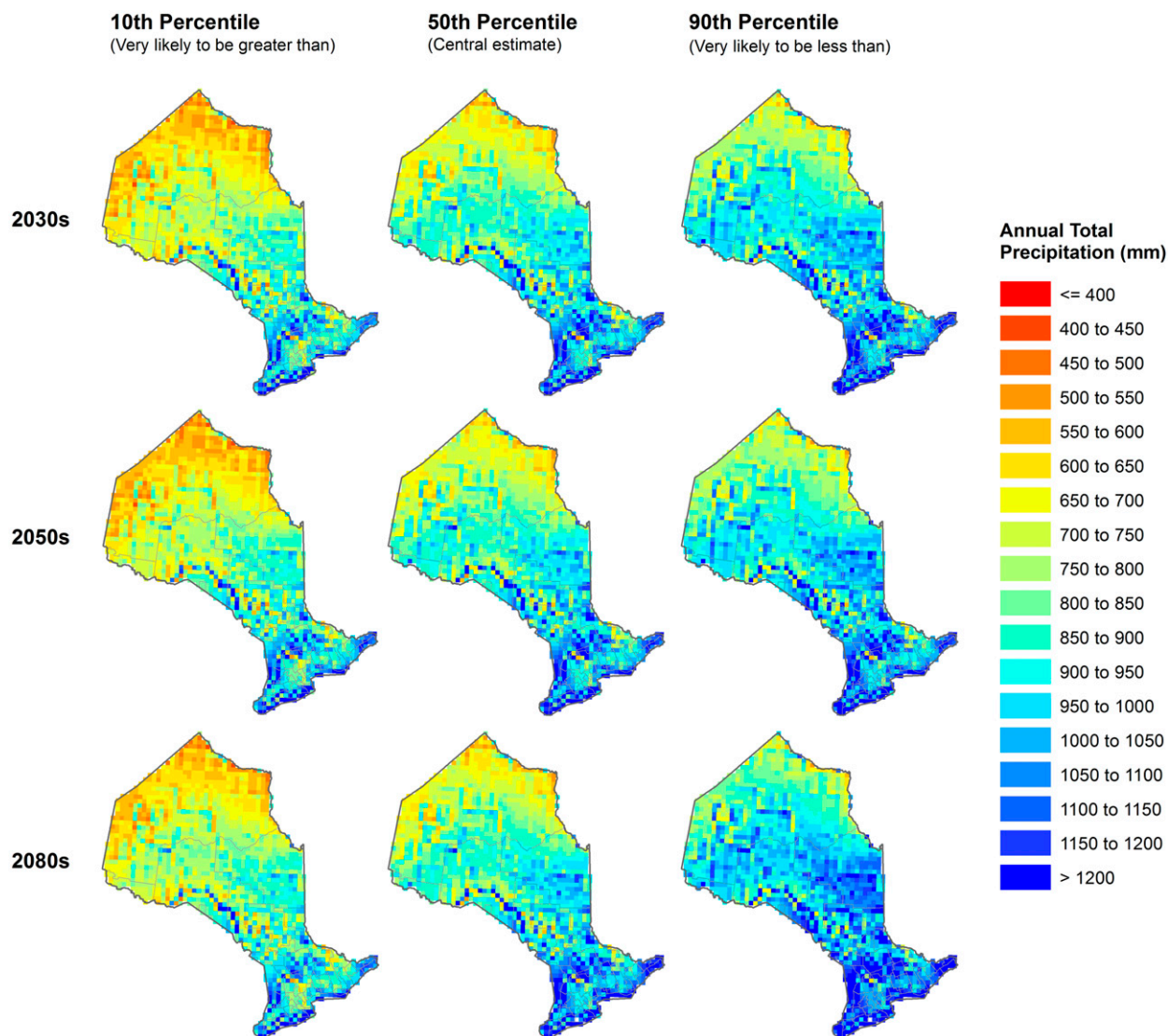


FIG. 10. As in Fig. 8, but for annual total precipitation.

[2.6, 2.7] $^{\circ}$ C in the 2030s, [4.0, 4.7] $^{\circ}$ C in the 2050s, and [5.9, 7.4] $^{\circ}$ C in the 2080s.

Figure 10 shows the projections of annual total precipitation over Ontario for three future periods at the 10th, 50th, and 90th percentiles. It can be found that there is an apparent spatially increasing pattern for annual total precipitation, like average temperature, along with the latitude. For example, the 50th percentiles of annual precipitation in the north would vary within [600, 800] mm in the 2030s, while in the middle and the south the projected annual precipitation in the same period would mostly be within [800, 1000] and [1000, 1200] mm, respectively. Furthermore, it seems that there are no significant changes in the spatial pattern of annual total precipitation (i.e., dry in the north and wet in the

south) in the 2050s and 2080s. To further investigate the temporal trend in annual precipitation, we extract the projected precipitation for the nine cities in three future periods and compare with the simulations for the baseline period. The results are presented in Fig. 11. Even though the changes in annual precipitation at these nine cities are distinct from each other, the vast majority of cities are projected to suffer positive changes varying within [3.2, 17.5]% in the future periods, except for the cities of Windsor and Kenora where negative changes in annual precipitation (within [−0.4, −3.4]%) are likely to occur. Because the magnitude of these negative changes is relatively small, it is reasonable to believe that there is likely to be a slight increasing trend in annual precipitation with time in the context of Ontario. In general,

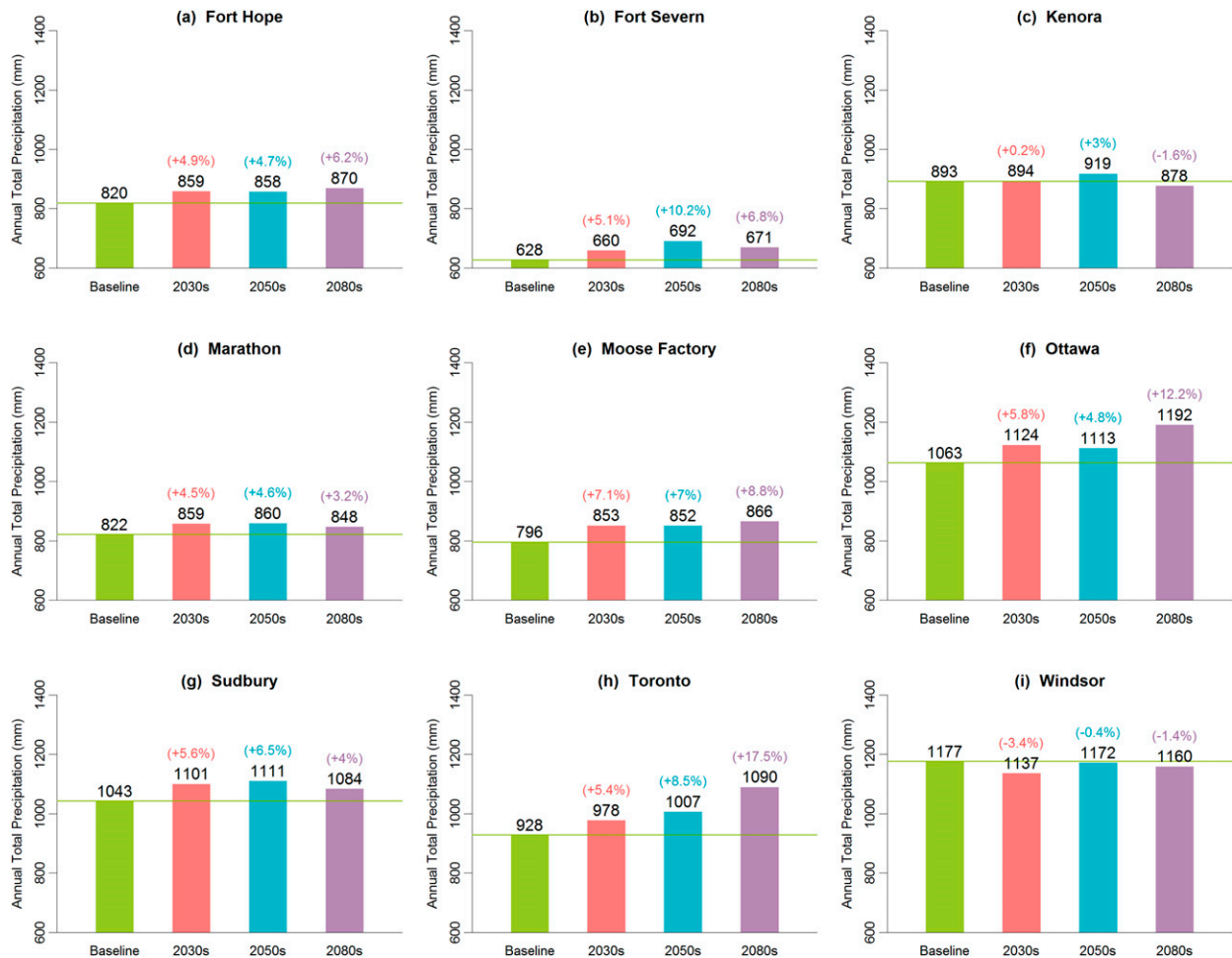


FIG. 11. As in Fig. 9, but for annual total precipitation.

the projected increase in annual precipitation would be [4.5, 7.1]% in the 2030s, [4.6, 10.2]% in the 2050s, and [3.2, 17.5]% in the 2080s.

In addition, projections of seasonal precipitation over Ontario are also analyzed in this study to help understand the annual cycle of precipitation (shown in Fig. 12). Apparent meridional patterns of seasonal precipitation (i.e., less in the north and more in the south) are also projected for winter, spring, and autumn (while no obvious spatial pattern is reported for summer). Meanwhile, an overall slight increasing trend in winter and spring precipitation is projected in most regions of the province. This is especially apparent for the northern areas where the grid cells with winter precipitation less than 100 mm or spring precipitation less than 150 mm are significantly reduced from the 2030s to 2080s. However, it seems that there are no obvious temporal trends in summer and autumn precipitation.

c. Projected IDF curves

Apart from high-resolution projections of a number of climate variables, Ontario CCDP also contains projections of IDF curves at 25-km gridpoint scales for the entire province. Because one IDF curve may include a great deal of information on the rainfall intensity under different combinations of duration and return period for extreme rainfall events, we present projections of IDF curves for only the nine selected cities in this paper (as illustrated in Fig. 13). The projected IDF curves for the entire province can be accessed and downloaded free of charge at Ontario CCDP for further analysis. The generated IDF curves for the baseline period have been validated at 12 selected stations in comparison with the ones developed with observational data provided by Environment Canada, and the validation results are presented in the paper of Wang et al. (2014c).

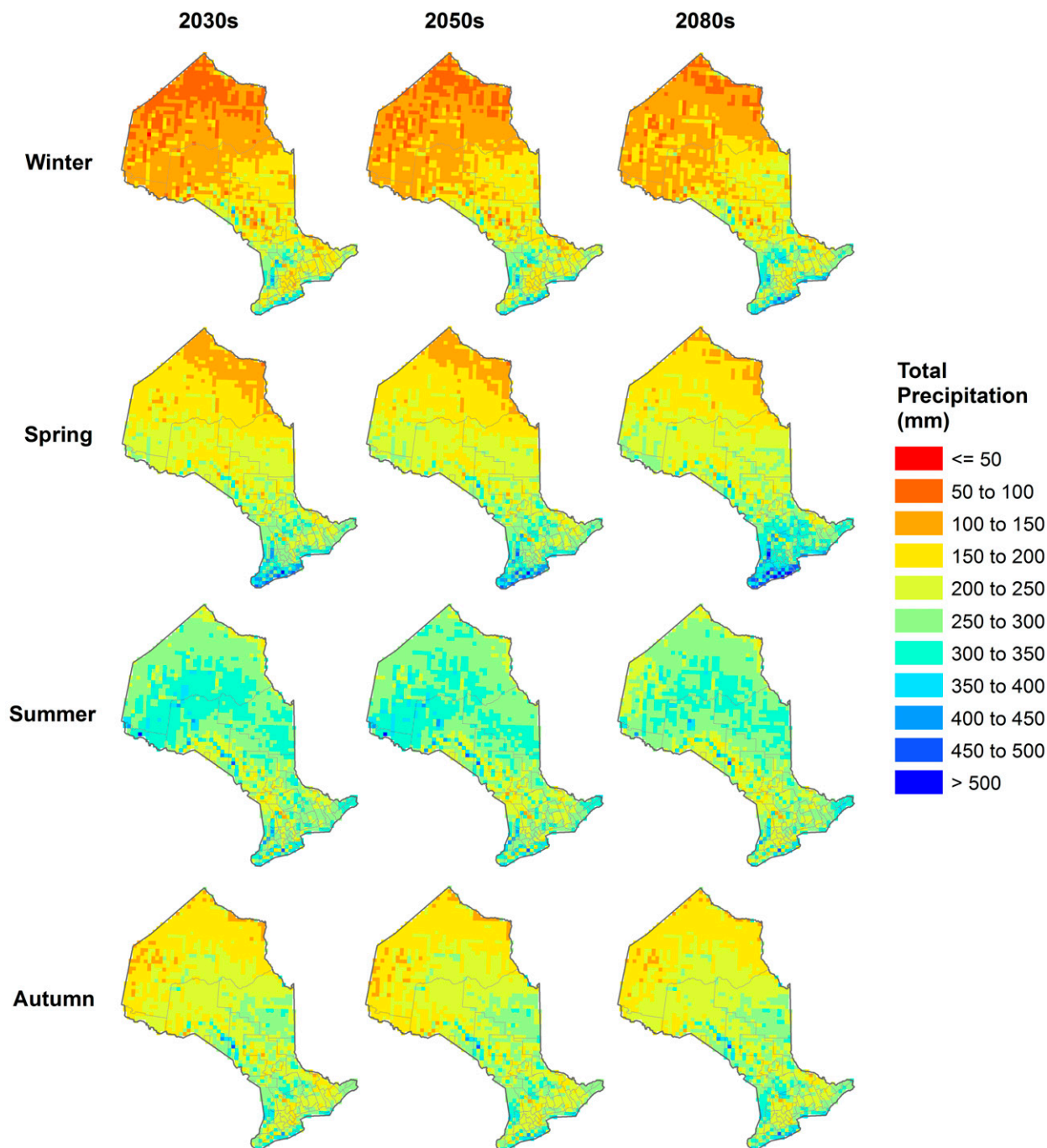


FIG. 12. Projections of seasonal precipitation for (top)–(bottom) winter, spring, summer, and autumn over Ontario (50th percentile) and (left)–(right) 2030s, 2050s, and 2080s.

Table 3 shows the 50th percentiles of rainfall intensity of 50- and 100-yr storms in the 2080s for the selected cities projected by the PRECIS ensemble simulations. Apparently, each city tells a totally different story in terms of the projected rainfall intensities at different durations and return periods because of the spatial

variations in precipitation. For example, the projected rainfall intensity for a 50-yr storm with a 24-h duration in Ottawa is likely to be the same as the one in Windsor (i.e., 7.4 mm h^{-1}), but the intensities for a 50-yr storm with a 1-h duration in these two cities are obviously different from each other (i.e., 65.7 mm h^{-1} in Ottawa

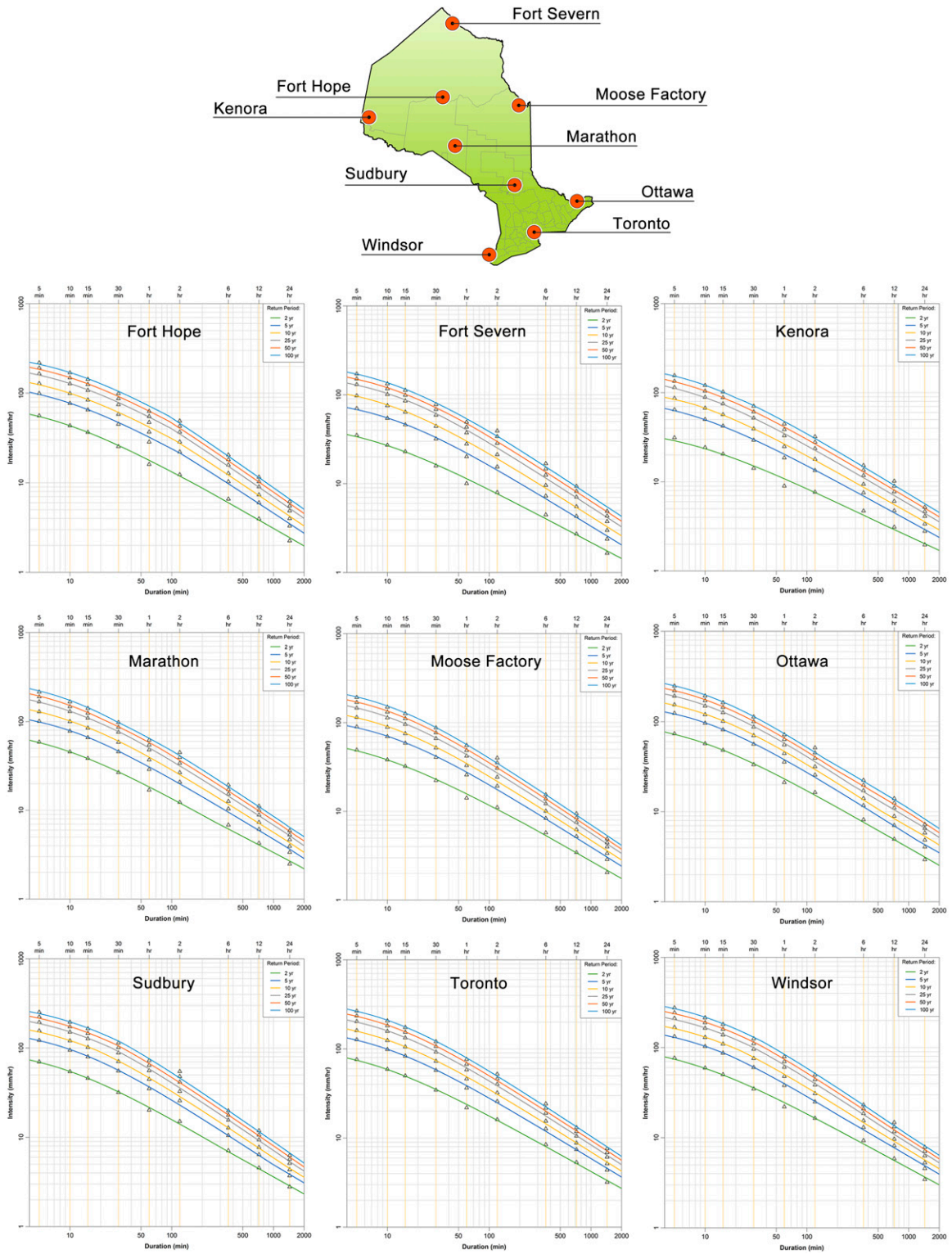


FIG. 13. Projected rainfall IDF curves in the 2080s at nine selected cities (50th percentile).

TABLE 3. Projected rainfall intensity of 50- and 100-yr storms in the 2080s for the selected cities (50th percentile; mm h^{-1}).

| City name | 50-yr return period | | | | | 100-yr return period | | | | |
|---------------|---------------------|------|------|------|------|----------------------|------|------|------|------|
| | 1 h | 2 h | 6 h | 12 h | 24 h | 1 h | 2 h | 6 h | 12 h | 24 h |
| Fort Hope | 63.0 | 40.6 | 17.5 | 10.2 | 5.9 | 72.0 | 46.2 | 19.8 | 11.4 | 6.6 |
| Fort Severn | 47.4 | 29.8 | 13.5 | 8.1 | 4.8 | 53.7 | 34.1 | 15.5 | 9.2 | 5.5 |
| Kenora | 41.2 | 26.7 | 12.9 | 8.1 | 5.1 | 47.7 | 30.7 | 14.7 | 9.2 | 5.7 |
| Marathon | 58.2 | 36.5 | 16.5 | 9.8 | 5.8 | 64.9 | 41.3 | 18.5 | 11.0 | 6.4 |
| Moose Factory | 50.2 | 31.0 | 13.8 | 8.2 | 4.8 | 56.7 | 34.9 | 15.4 | 9.1 | 5.3 |
| Ottawa | 65.7 | 40.8 | 19.2 | 12.1 | 7.4 | 73.7 | 45.6 | 21.8 | 13.7 | 8.3 |
| Sudbury | 67.3 | 41.0 | 17.8 | 10.4 | 6.0 | 76.1 | 46.2 | 19.9 | 11.6 | 6.7 |
| Toronto | 70.4 | 44.0 | 20.0 | 12.0 | 7.2 | 79.3 | 49.5 | 22.4 | 13.4 | 8.0 |
| Windsor | 74.3 | 45.9 | 20.6 | 12.2 | 7.4 | 84.3 | 51.8 | 23.0 | 13.6 | 8.1 |

and 74.3 mm h^{-1} in Windsor). However, we note that there is an increasing tendency of the projected rainfall intensity along with the latitude. In other words, the projected rainfall storms in southern cities are usually more intensive than those in northern cities. For example, intensities of a 100-yr rainfall storm with a 24-h duration in Ottawa, Toronto, and Windsor are all likely to be 8 mm h^{-1} or even higher, while the rainfall intensities under the same return period and duration in Fort Severn, Fort Hope, and Moose Factory are all projected to be lower than 7 mm h^{-1} .

To analyze the temporal trend in the intensity of rainfall storms, we further extract the rainfall intensities with a 100-yr return period and a 24-h duration for the baseline and future periods at the nine cities. The percentage changes in the rainfall intensity of storm events in three future periods relative to the baseline period are then computed. The results are shown in Fig. 14. It seems that most of the cities are likely to suffer an increase in the intensity of a 100-yr rainfall storm with a 24-h duration because the overwhelming majority of percentage changes are positive while negative changes are likely to occur only in Kenora and Moose Factory during the 2030s (by -4.7% and -3% , respectively), in Fort Hope during the 2050s (by -2.6%), and in Windsor during the 2080s (by -6.4%). However, the magnitude of these negative changes is relatively small in comparison with the projected positive changes (mostly higher than 15%). This may suggest that there is likely to be an overall increase in the projected rainfall intensity from the 2030s to 2080s at most of the selected cities, although the projected intensity in the 2050s at a few cities may be temporally strengthened (e.g., in Marathon) or weakened (e.g., in Sudbury).

5. Summary and conclusions

In this study, high-resolution regional climate projections over Ontario, Canada, were developed through an ensemble modeling approach to provide reliable and

ready-to-use climate scenarios for assessing plausible effects of future climatic changes at local scales. We adopted the PRECIS regional climate modeling system to conduct ensemble simulations in a continuous run from 1950 to 2099, which was driven by the boundary conditions from a HadCM3-based perturbed physics ensemble. The ensemble simulations were divided into four time slices including one baseline period and three future periods (i.e., 2030s, 2050s, and 2080s). Simulations of temperature and precipitation for the baseline period were compared to the observed values to validate the performance of the ensemble in capturing the current climatology over Ontario. Future projections were then analyzed to help understand plausible changes in its local climate in response to global warming. To make the ensemble projections available to the general public, a web-based climate data portal named Ontario CCDP was developed (<http://ontarioccdp.ca>). The Ontario CCDP contains a number of representative climate variables, such as temperature, precipitation, humidity, solar radiation, wind speed, and wind direction. Additionally, we have developed the projections of rainfall IDF curves to help understand the possible effects of climate change on extreme precipitation events in the context of Ontario. The projected IDF curves at 25-km gridpoint scales were also made available at Ontario CCDP.

Our analyses for the climate projections over Ontario indicate that there is likely to be an obvious warming trend with time over the entire province. This is especially true for the northern end where the central estimate of average temperature is projected to be below zero (i.e., $[-2, 0]^\circ\text{C}$) in the 2030s; afterward the average temperature is likely to rise above zero (i.e., $[0, 2]^\circ\text{C}$) in the 2050s and would continue to increase up to $[3, 5]^\circ\text{C}$ in the 2080s. We also find that the spatial variability in the magnitude of temperature increase is very little even though there is an apparent increasing pattern from north to south in the average temperature. For the whole province, the average temperature is likely to increase by $[2.6, 2.7]^\circ\text{C}$ in the

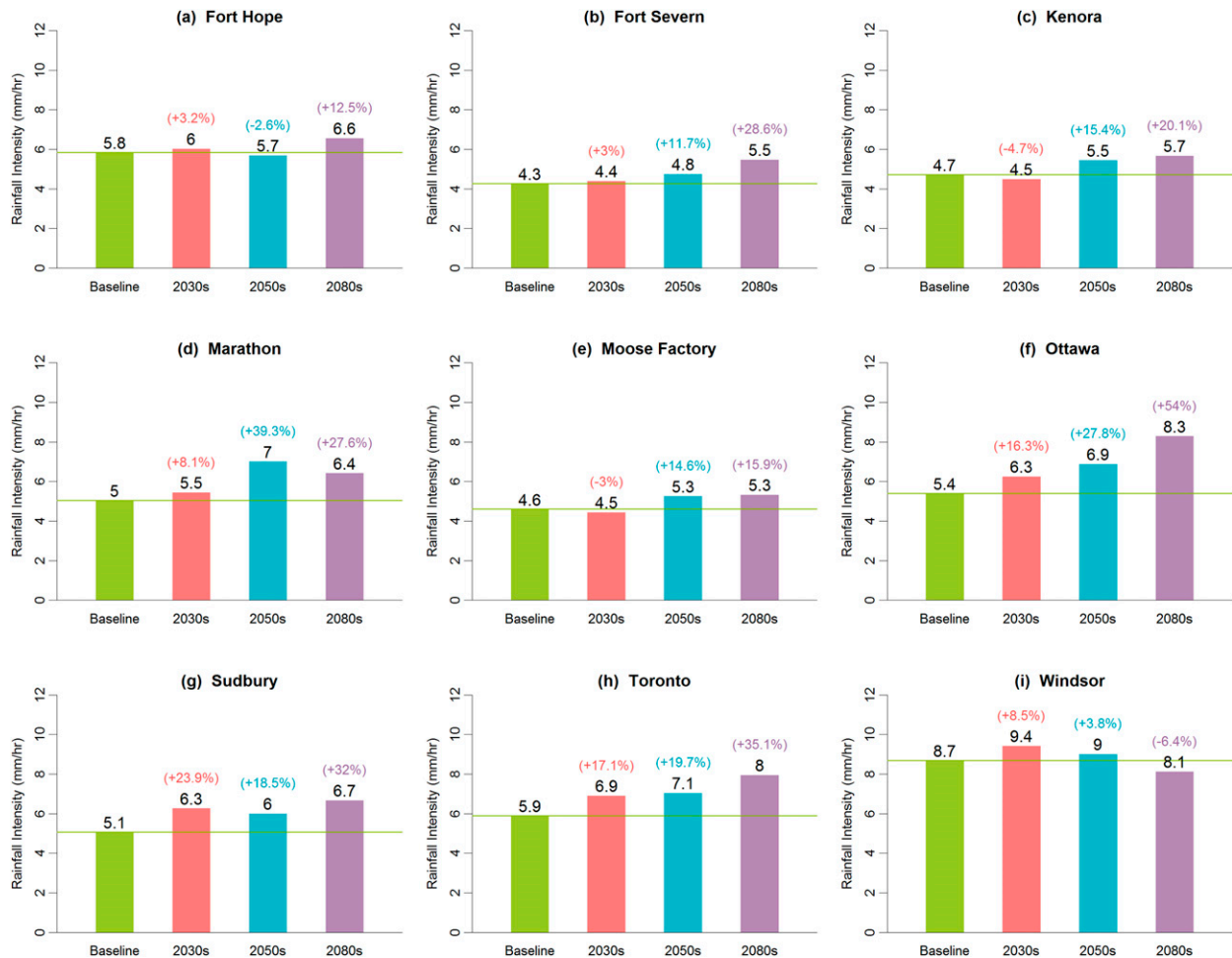


FIG. 14. As in Fig. 9, but for rainfall intensity for the storm event with 24-h duration and 100-yr return period (50th percentile).

2030s, [4.0, 4.7] $^{\circ}$ C in the 2050s, and [5.9, 7.4] $^{\circ}$ C in the 2080s. Likewise, the annual total precipitation over the entire province is projected to increase slightly (i.e., [4.5, 7.1]% in the 2030s, [4.6, 10.2]% in the 2050s, and [3.2, 17.5]% in the 2080s). The projected increase in annual precipitation is mainly contributed by the increases in winter and spring precipitation as there are no obvious temporal trends in summer and autumn precipitation. Furthermore, our analyses of the projected IDF curves suggest that there is likely to be an overall increase in the intensity of rainfall storms at most of the cities in Ontario.

Since its initial launch on January 2014, Ontario CCDP has received about 16 000 downloading requests from over 150 registered users (as of June 2015), including academia, municipal and provincial agencies, nongovernment agencies, and private sectors. The climate data included in Ontario CCDP have been widely used for different research purposes, such as agricultural impact and risk assessments, water quality and quantity

forecasting, infrastructure design and operations, wind power applications, analysis of the impacts of the shrinking ice cover over the Great Lakes and Hudson Bay, and many other applications related to climate change impact assessment and adaptation studies. However, we should note that the climate data and IDF curves contained in the current version of Ontario CCDP are all based upon the projections from phase 3 of the Coupled Model Intercomparison Project (CMIP3). Along with the release of phase 5 of CMIP (CMIP5) by the World Climate Research Programme's Working Group on Coupled Modelling in 2011, a state-of-the-art multimodel dataset was produced with the advancement of human knowledge in climate systems. Our ongoing efforts are therefore updating the high-resolution climate projections for the province of Ontario through ensemble downscaling to the CMIP5 dataset. Continuing developments and improvements to the data portal are also part of our future efforts. Following that, more climate projections and analysis

tools will be developed and integrated into the next version of Ontario CCDP.

Acknowledgments. The climate projections and IDF curves used in this article are all obtained from Ontario CCDP (<http://ontarioccdp.ca>). This research was supported by the Natural Sciences Foundation (51190095, 51225904), the Program for Innovative Research Team in University (IRT1127), the Ontario Ministry of the Environment and Climate Change, and the Natural Science and Engineering Research Council of Canada.

REFERENCES

- Bellprat, O., S. Kotlarski, D. Lüthi, and C. Schär, 2012: Exploring perturbed physics ensembles in a regional climate model. *J. Climate*, **25**, 4582–4599, doi:10.1175/JCLI-D-11-00275.1.
- Bierbaum, R., and Coauthors, 2013: A comprehensive review of climate adaptation in the United States: More than before, but less than needed. *Mitigation Adapt. Strategies Global Change*, **18**, 361–406, doi:10.1007/s11027-012-9423-1.
- Borga, M., C. Vezzani, and G. Dalla Fontana, 2005: Regional rainfall depth–duration–frequency equations for an alpine region. *Nat. Hazards*, **36**, 221–235, doi:10.1007/s11069-004-4550-y.
- Brown, C., and R. L. Wilby, 2012: An alternate approach to assessing climate risks. *Eos, Trans. Amer. Geophys. Union*, **93**, 401–402, doi:10.1029/2012EO410001.
- Carlsson-Kanyama, A., H. Carlsen, and K.-H. Dreborg, 2013: Barriers in municipal climate change adaptation: Results from case studies using backcasting. *Futures*, **49**, 9–21, doi:10.1016/j.futures.2013.02.008.
- Castro, C. L., R. A. Pielke, G. Leoncini, 2005: Dynamical downscaling: Assessment of value retained and added using the Regional Atmospheric Modeling System (RAMS). *J. Geophys. Res.*, **110**, D05108, doi:10.1029/2004JD004721.
- Chen, H.-L., and A. R. Rao, 2002: Testing hydrologic time series for stationarity. *J. Hydrol. Eng.*, **7**, 129–136, doi:10.1061/(ASCE)1084-0699(2002)7:2(129).
- Cheung, W. W. L., V. W. Y. Lam, J. L. Sarmiento, K. Kearney, R. Watson, and D. Pauly, 2009: Projecting global marine biodiversity impacts under climate change scenarios. *Fish Fish.*, **10**, 235–251, doi:10.1111/j.1467-2979.2008.00315.x.
- Collins, M., B. B. Booth, G. R. Harris, J. M. Murphy, D. M. Sexton, and M. J. Webb, 2006: Towards quantifying uncertainty in transient climate change. *Climate Dyn.*, **27**, 127–147, doi:10.1007/s00382-006-0121-0.
- Crossman, J., M. Futter, S. Oni, P. Whitehead, L. Jin, D. Butterfield, H. Baulch, and P. Dillon, 2013: Impacts of climate change on hydrology and water quality: Future proofing management strategies in the Lake Simcoe watershed, Canada. *J. Great Lakes Res.*, **39**, 19–32, doi:10.1016/j.jglr.2012.11.003.
- Diro, G., A. Tompkins, and X. Bi, 2012: Dynamical downscaling of ECMWF ensemble seasonal forecasts over East Africa with RegCM3. *J. Geophys. Res.*, **117**, D16103, doi:10.1029/2011JD016997.
- Doney, S. C., and Coauthors, 2012: Climate change impacts on marine ecosystems. *Annu. Rev. Mar. Sci.*, **4**, 11–37, doi:10.1146/annurev-marine-041911-111611.
- Fowler, H., S. Blenkinsop, and C. Tebaldi, 2007: Linking climate change modelling to impacts studies: Recent advances in downscaling techniques for hydrological modelling. *Int. J. Climatol.*, **27**, 1547–1578, doi:10.1002/joc.1556.
- Haines, A., R. S. Kovats, D. Campbell-Lendrum, and C. Corvalan, 2006: Climate change and human health: Impacts, vulnerability and public health. *Public Health*, **120**, 585–596, doi:10.1016/j.puhe.2006.01.002.
- Hansen, J., M. Sato, and R. Ruedy, 2012: Perception of climate change. *Proc. Natl. Acad. Sci. USA*, **109**, E2415–E2423, doi:10.1073/pnas.1205276109.
- Harley, C. D. G., and Coauthors, 2006: The impacts of climate change in coastal marine systems. *Ecol. Lett.*, **9**, 228–241, doi:10.1111/j.1461-0248.2005.00871.x.
- He, J., C. Valeo, and F. Bouchart, 2006: Enhancing urban infrastructure investment planning practices for a changing climate. *Water Sci. Technol.*, **53**, 13–20, doi:10.2166/wst.2006.292.
- , —, A. Chu, and N. F. Neumann, 2011: Stormwater quantity and quality response to climate change using artificial neural networks. *Hydrol. Processes*, **25**, 1298–1312, doi:10.1002/hyp.7904.
- , A. Anderson, and C. Valeo, 2015: Bias compensation in flood frequency analysis. *Hydrol. Sci. J.*, **60**, 381–401, doi:10.1080/02626667.2014.885651.
- Hirabayashi, Y., R. Mahendran, S. Koirala, L. Konoshima, D. Yamazaki, S. Watanabe, H. Kim, and S. Kanae, 2013: Global flood risk under climate change. *Nat. Climate Change*, **3**, 816–821, doi:10.1038/nclimate1911.
- Hogg, W. D., D. Carr, B. Routledge, 1989: Rainfall intensity-duration frequency values for Canadian locations. Environment Canada Atmospheric Environment Service Rep., 17 pp.
- Hyndman, R. J., and Y. Fan, 1996: Sample quantiles in statistical packages. *Amer. Stat.*, **50**, 361–365.
- IPCC, 2000: Summary for policymakers. *Special Report on Emissions Scenarios*, N. Nakicenovic and R. Swart, Eds., Cambridge University Press, 1–20. [Available online at <https://www.ipcc.ch/pdf/special-reports/spm/sres-en.pdf>.]
- , 2014: Summary for policymakers. *Climate Change 2014: Synthesis Report*, R. K. Pachauri et al., Eds., Cambridge University Press, 1–31. [Available online at http://www.ipcc.ch/pdf/assessment-report/ar5/syr/AR5_SYR_FINAL_SPM.pdf.]
- Jha, S. K., G. Mariethoz, J. P. Evans, and M. F. McCabe, 2013: Demonstration of a geostatistical approach to physically consistent downscaling of climate modeling simulations. *Water Resour. Res.*, **49**, 245–259, doi:10.1029/2012WR012602.
- Jones, H. P., D. G. Hole, and E. S. Zavaleta, 2012: Harnessing nature to help people adapt to climate change. *Nat. Climate Change*, **2**, 504–509, doi:10.1038/nclimate1463.
- Jones, R. G., M. Noguer, D. C. Hassell, D. Hudson, S. S. Wilson, G. J. Jenkins, and J. F. B. Mitchell, 2004: Generating high resolution climate change scenarios using PRECIS. UNDP/Met Office Hadley Centre Rep., 40 pp. [Available online at http://www.metoffice.gov.uk/media/pdf/6/5/PRECIS_Handbook.pdf.]
- Jordan, Y. C., A. Ghulam, and M. L. Chu, 2014: Assessing the impacts of future urban development patterns and climate changes on total suspended sediment loading in surface waters using geoinformatics. *J. Environ. Inf.*, **24**, 65–79.
- Ling, J., M. L. Wu, Y. F. Chen, Y. Y. Zhang, and J. D. Dong, 2014: Identification of spatial and temporal patterns of coastal waters in Sanya Bay, South China Sea by chemometrics. *J. Environ. Inf.*, **23**, 37–43, doi:10.3808/jei.201400255.
- Ma, Z. Z., Z. J. Wang, T. Xia, C. J. Gippel, and R. Speed, 2014: Hydrograph-based hydrologic alteration assessment and its application to the Yellow River. *J. Environ. Inf.*, **23**, 1–13, doi:10.3808/jei.201400252.
- Madsen, H., P. S. Mikkelsen, D. Rosbjerg, and P. Harremoës, 2002: Regional estimation of rainfall intensity-duration-frequency

- curves using generalized least squares regression of partial duration series statistics. *Water Resour. Res.*, **38**, 1239, doi:10.1029/2001WR001125.
- , K. Arnbjerg-Nielsen, and P. S. Mikkelsen, 2009: Update of regional intensity–duration–frequency curves in Denmark: Tendency towards increased storm intensities. *Atmos. Res.*, **92**, 343–349, doi:10.1016/j.atmosres.2009.01.013.
- Mailhot, A., S. Duchesne, D. Caya, and G. Talbot, 2007: Assessment of future change in intensity–duration–frequency (IDF) curves for southern Quebec using the Canadian Regional Climate Model (CRCM). *J. Hydrol.*, **347**, 197–210, doi:10.1016/j.jhydrol.2007.09.019.
- McMichael, A. J., R. E. Woodruff, and S. Hales, 2006: Climate change and human health: Present and future risks. *Lancet*, **367**, 859–869, doi:10.1016/S0140-6736(06)68079-3.
- McSweeney, C. F., and R. G. Jones, 2010: Selecting members of the ‘QUMP’ perturbed-physics ensemble for use with PRECIS. Met Office Hadley Centre Rep., 8 pp. [Available online at <http://www.metoffice.gov.uk/media/pdf/e/3/SelectingCGMsToDownscale.pdf>.]
- , —, and B. B. Booth, 2012: Selecting ensemble members to provide regional climate change information. *J. Climate*, **25**, 7100–7121, doi:10.1175/JCLI-D-11-00526.1.
- Murphy, J. M., and Coauthors, 2009: UK climate projections: Climate change projections. Met Office Hadley Centre Rep. UKCP09, 190 pp. [Available online at <http://ukclimateprojections.metoffice.gov.uk/media.jsp?mediaid=87894&filetype=pdf>.]
- NLWIS, 2007: Daily 10 km raster-gridded climate dataset for Canada 1961–2003, version 1.0. National Land and Water Information Service, Agriculture and Agri-Food Canada, accessed 10 December 2014. [Available online at <https://www.mcgill.ca/library/find/maps/dgcd10km>.]
- Ontario Ministry of the Environment, 2011a: Climate action: Adapting to change, protecting our future. Ontario Ministry of the Environment Rep. PIBS 8291e, 13 pp. [Available online at <http://www.climateontario.ca/doc/publications/ClimateAction-AdaptingToChangeProtectingOurFuture2011.pdf>.]
- , 2011b: Climate ready: Ontario’s adaptation strategy and action plan. Ontario Ministry of the Environment Rep. PIBS 8292e, 120 pp. [Available online at http://www.abca.on.ca/downloads/MOE_Climate_Ready_ENG.pdf.]
- Parmesan, C., and G. Yohe, 2003: A globally coherent fingerprint of climate change impacts across natural systems. *Nature*, **421**, 37–42, doi:10.1038/nature01286.
- Patz, J. A., D. Campbell-Lendrum, T. Holloway, and J. A. Foley, 2005: Impact of regional climate change on human health. *Nature*, **438**, 310–317, doi:10.1038/nature04188.
- Piao, S., and Coauthors, 2010: The impacts of climate change on water resources and agriculture in China. *Nature*, **467**, 43–51, doi:10.1038/nature09364.
- Pierce, D. W., and Coauthors, 2013: Probabilistic estimates of future changes in California temperature and precipitation using statistical and dynamical downscaling. *Climate Dyn.*, **40**, 839–856, doi:10.1007/s00382-012-1337-9.
- Poloczanska, E. S., and Coauthors, 2013: Global imprint of climate change on marine life. *Nat. Climate Change*, **3**, 919–925, doi:10.1038/nclimate1958.
- Rife, D. L., E. Vanyvyve, J. O. Pinto, A. J. Monaghan, C. A. Davis, and G. S. Poulos, 2013: Selecting representative days for more efficient dynamical climate downscaling: Application to wind energy. *J. Appl. Meteor. Climatol.*, **52**, 47–63, doi:10.1175/JAMC-D-12-016.1.
- Robinson, K., C. Valeo, M. Ryan, A. Chu, and M. Iwanyszyn, 2009: Modelling aquatic vegetation and dissolved oxygen after a flood event in the Bow River, Alberta, Canada. *Can. J. Civ. Eng.*, **36**, 492–503, doi:10.1139/L08-126.
- Schmidli, J., C. Frei, and P. L. Vidale, 2006: Downscaling from GCM precipitation: A benchmark for dynamical and statistical downscaling methods. *Int. J. Climatol.*, **26**, 679–689, doi:10.1002/joc.1287.
- Surampalli, R. Y., T. C. Zhang, C. Ojha, R. Tyagi, and C. Kao, 2013: *Climate Change Modeling, Mitigation, and Adaptation*. American Society of Civil Engineers, 728 pp.
- Valeo, C., Z. Xiang, F.-C. Bouchart, P. Yeung, and M. Ryan, 2007: Climate change impacts in the Elbow River watershed. *Can. Water Resour. J.*, **32**, 285–302, doi:10.4296/cwrj3204285.
- Van Vuuren, D. P., and Coauthors, 2011: The representative concentration pathways: An overview. *Climatic Change*, **109**, 5–31, doi:10.1007/s10584-011-0148-z.
- Veneziano, D., and P. Furcolo, 2002: Multifractality of rainfall and scaling of intensity-duration-frequency curves. *Water Resour. Res.*, **38**, 1306, doi:10.1029/2001WR000372.
- Wang, L. Z., Y. F. Huang, L. Wang, and G. Q. Wang, 2014: Pollutant flushing characterizations of stormwater runoff and their correlation with land use in a rapidly urbanizing watershed. *J. Environ. Inf.*, **23**, 44–54, doi:10.3808/jei.201400256.
- Wang, X., and Coauthors, 2013: A stepwise cluster analysis approach for downscaled climate projection—A Canadian case study. *Environ. Modell. Software*, **49**, 141–151, doi:10.1016/j.envsoft.2013.08.006.
- , G. Huang, Q. Lin, and J. Liu, 2014a: High-resolution probabilistic projections of temperature changes over Ontario, Canada. *J. Climate*, **27**, 5259–5284, doi:10.1175/JCLI-D-13-00717.1.
- , —, —, X. Nie, and J. Liu, 2014b: High-resolution temperature and precipitation projections over Ontario, Canada: A coupled dynamical-statistical approach. *Quart. J. Roy. Meteor. Soc.*, **141**, 1137–1146, doi:10.1002/qj.2421.
- , —, and J. Liu, 2014c: Projected increases in intensity and frequency of rainfall extremes through a regional climate modeling approach. *J. Geophys. Res. Atmos.*, **119**, 13 271–13 286, doi:10.1002/2014JD022564.
- , —, and —, 2015: Projected increases in near-surface air temperature over Ontario, Canada: A regional climate modeling approach. *Climate Dyn.*, doi:10.1007/s00382-014-2387-y, in press.
- Wende, W., A. Bond, N. Bobylev, and L. Stratmann, 2012: Climate change mitigation and adaptation in strategic environmental assessment. *Environ. Impact Assess. Rev.*, **32**, 88–93, doi:10.1016/j.eiar.2011.04.003.
- Whitehead, P., R. Wilby, R. Battarbee, M. Kernan, and A. J. Wade, 2009: A review of the potential impacts of climate change on surface water quality. *Hydrol. Sci. J.*, **54**, 101–123, doi:10.1623/hysj.54.1.101.
- Willems, P., K. Arnbjerg-Nielsen, J. Olsson, and V. Nguyen, 2012: Climate change impact assessment on urban rainfall extremes and urban drainage: Methods and shortcomings. *Atmos. Res.*, **103**, 106–118, doi:10.1016/j.atmosres.2011.04.003.
- Wilson, S., D. Hassell, D. Hein, C. Morrell, S. Tucker, R. Jones, and R. Taylor, 2011: Installing and using the Hadley Centre regional climate modelling system, PRECIS. Met Office Hadley Centre Rep., 157 pp. [Available online at http://www.metoffice.gov.uk/media/pdf/o/5/tech_man_vn1.9.3.pdf.pdf.]
- Yang, W., and Z. F. Yang, 2014: Evaluation of sustainable environmental flows based on the valuation of ecosystem services: A case study for the Baiyangdian Wetland, China. *J. Environ. Inf.*, **24**, 90–100, doi:10.3808/jei.201400276.

Copyright of Journal of Climate is the property of American Meteorological Society and its content may not be copied or emailed to multiple sites or posted to a listserv without the copyright holder's express written permission. However, users may print, download, or email articles for individual use.